Remote Sensing of Environment 159 (2015) 278–287

Contents lists available at ScienceDirect

Remote Sensing of Environment

journal homepage: www.elsevier.com/locate/rse

Satellite observation of hourly dynamic characteristics of algae with Geostationary Ocean Color Imager (GOCI) data in Lake Taihu

Changchun Huang [a,b,f], Kun Shi [c], Hao Yang [a], Yunmei Li [a,b,*], A-xing Zhu [a,b,d], Deyong Sun [e], Liangjiang Xu [a], Jun Zou [a], Xia Chen [a]

[a] Key Laboratory of Virtual Geographic Environment (Nanjing Normal University), Ministry of Education, Nanjing 210046, China
[b] Jiangsu Center for Collaborative Innovation in Geographical Information Resource Development and Application, Nanjing Normal University, Nanjing 210023, China
[c] Nanjing Institute of Geography and Limnology, Chinese Academy of Sciences, Nanjing 210046, China
[d] Department of Geography, University of Wisconsin, Madison, WI 53706, USA
[e] College of Remote Sensing, Nanjing University of Information Science & Technology, Nanjing 210046, China
[f] Jiangsu Provincial Key Laboratory of Materials Cycling and Pollution Control, Nanjing Normal University, Nanjing 210023, China

ARTICLE INFO

Article history:
Received 1 August 2014
Received in revised form 18 December 2014
Accepted 22 December 2014
Available online 16 January 2015

Keywords:
Chlorophyll-a concentration
NIR-red algorithm
Taihu Lake
Algal bloom

ABSTRACT

Phytoplankton bloom in a shallow inland eutrophic lake (Taihu Lake) is characterized by significant spatial and temporal variation and a high concentration of chlorophyll-a ($C_{chl\text{-}a}$). The observation of the rapidly changing dynamic characteristics of algae is limited by the insufficient temporal resolution of satellite data. The Geostationary Ocean Color Imager (GOCI), launched by Korea, can provide high temporal resolution satellite data to observe the hourly dynamics of algae. In this study, a simple regional NIR-red two-band empirical algorithm of $C_{chl\text{-}a}$ for GOCI is proposed for Taihu Lake. Study results show that the GOCI-derived $C_{chl\text{-}a}$ matches the in situ measured values well. Based on this validated algorithm of $C_{chl\text{-}a}$, we obtained the hourly maps of $C_{chl\text{-}a}$ from GOCI level-1b data during the period August 6 to August 9, 2013. The spatial variation of GOCI-derived $C_{chl\text{-}a}$ also matches synchronous in situ measured values well, and the temporal variation of GOCI-derived $C_{chl\text{-}a}$ coincides with buoy-measured $C_{chl\text{-}a}$. The northwestern area of the lake and Meiliang Bay are worst hit by phytoplankton bloom. GOCI-derived $C_{chl\text{-}a}$ revealed a clear evidence of hourly spatial and temporal variations of $C_{chl\text{-}a}$ in Taihu Lake. The vertical current plays an important role in the hourly scale of spatial and temporal variations in phytoplankton. The horizontal current is important to the distribution of phytoplankton over the long term, but spatially and temporally limited in the short term.

1. Introduction

Algae are vital to marine and freshwater ecosystems because of their key role in keeping the biosphere balanced despite natural forces and food-chain relationships (Cloern, 2001; Rabalais, 2004). Algal blooms, however, which are formed from the excessive growth of algae in freshwater and coastal marine ecosystems, are caused by increased nutrients (i.e., nitrogen and phosphorus) and have become a global problem. Algal blooms (such as *Microcystis aeruginosa*, *Scenedesmus obliquus* and diatom) occur worldwide. Taihu, Dianchi and Chaohu Lakes in China (Huang, Li, Yang, Sun, et al., 2014; Huang, Wang, et al., 2014; Paerl et al., 2011), Lake Erie in the United States (Michalak et al., 2013; Stumpf, Wynne, Baker, & Fahnenstiel, 2012), Lakes Wood and Winnipeg in Canada (Binding, Greenberg, & Bukata, 2011; Schindler, Hecky, & McCullough, 2012), and Lake Nieuwe Meer in the Netherlands (Jöhnk et al., 2008), have received much attention for their harmful toxins. The blooms are generally perceived to result from a rapid increase in biomass, because the algae growth period is much longer than the loss period. Previous studies have proposed that the intensity and frequency of blooms are empirically connected to nutrient status (Abell, Ozkundakci, & Hamilton, 2010; Paerl et al., 2011; Schindler et al., 2008; Xu, Paerl, Qin, Zhu, & Gao, 2010). Temperature, light and water dynamic characteristics are also important influencing factors (Carstensen, Henriksen, & Heiskanen, 2007; Moore et al., 2008; Paerl & Huisman, 2009; Wong, Lee, & Hodgkiss, 2007; Zhang, Duan, Shi, Yu, & Kong, 2012). The formation process of algal bloom is clearly complex.

Indeed, regulating nutrient input is the only realistic method of controlling algal bloom intensity and frequency (Conley et al., 2009; Paerl et al., 2011). As an extremely eutrophic lake, the nutrient input into the Taihu Lake watershed was effectively controlled, but the dynamic release of nutrients from sediment was not. (Dzialowski, Wang, Lim, Beury, & Huggins, 2008; Qin, Xu, Wu, Luo, & Zhang, 2007; Qin et al., 2006). Consequently, eutrophication could not be controlled in a short time period. However, the high rates of algal blooms create an urgent need for effective measures to reduce loss caused by blooms.

* Corresponding author at: Department of Geography, Nanjing Normal University, Wenyuan Road 1#, Qixia, Nanjing City, Jiangsu Province, China. Tel.: +86 25 85891740; fax: +86 25 85891623.
E-mail address: huangchangchun_aaa@163.com (C. Huang).

http://dx.doi.org/10.1016/j.rse.2014.12.016
0034-4257/

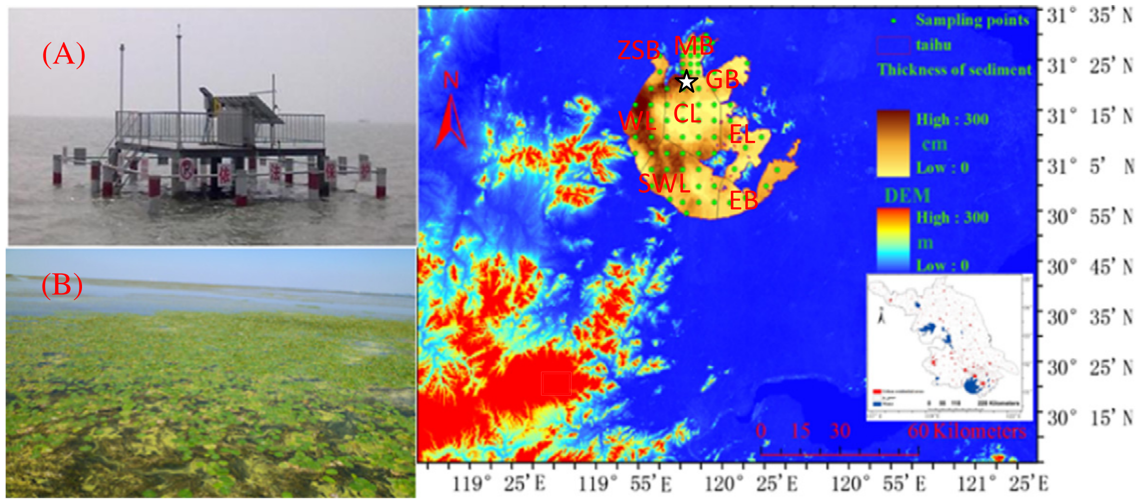

Fig. 1. Study area. The bottom right corner is the location of Taihu Lake in Jiangsu province. The black star is the position of buoy. The background of Taihu Lake is thickness of sediment. Taihu Lake can be separated into seven segments, including: Meiliang Bay (MB), Central Lake (CL), Gonghu Lake (GL), Western Lake (WL), Southwestern Lake (SWL), Eastern Lake (EL) and Eastern Bay (EB), Zhushan Bay (ZSB). A is a photo of the buoy. The main portion of the Eastern Bay is characterized by emergent aquatic plants, such as those shown in chart B.

Monitoring algal bloom and chlorophyll-a to evaluate and predict algal bloom is thus a critical prerequisite to finding effective methods to control the bloom. Satellite remote sensing provides rapid, synoptic, and repeated information on water quality (Duan et al., 2009; Hunter, Tyler, Willby, & Gilvear, 2008a, 2008b; Liu, Wang, & Shi, 2009; Odermatt et al., 2012). Many retrieval algorithms, such as the float algal index (Gower, King, Borstad, & Brown, 2005; Hu, 2009; Hu et al., 2005; Wynne, Stumpf, Tomlinson, & Dyble, 2010) and new chlorophyll-a retrieval models (Huang, Li, Yang, Li, et al., 2014; Shanmugam, 2011), have been developed to study the algal bloom, biological, and ecological processes and phenomena in Taihu Lake (Duan et al., 2009; Hu et al., 2010; Huang, Li, Yang, Li, et al., 2014; Le et al., 2009). Long-term records of algal blooms in the lake based on satellite data have been established to reveal large temporal and spatial variation of algal bloom (Duan et al., 2009; Hu et al., 2010; Wang, Shi, & Tang, 2011). However, there has been little published work on the dynamic characteristics of algae observation based on satellite data. This is due to the challenge of obtaining high temporal resolution, accurate atmospheric correction algorithms and a chlorophyll-a retrieval model for the satellite data. Hydrodynamic force has a significant effect on the formation of algal blooms and on their distribution (Moreno-Ostos, Cruz-Pizarro, Basanta, & George, 2009; Wu & Kong, 2009; Wu et al., 2013). This is particularly true for Taihu Lake because it is a shallow inland lake with a high dynamic ratio ([square root of the area]/depth: 25.4) (Huang, Li, Yang, Sun, et al., 2014), where algal (mainly is *M. aentginosa*) blooms occur every year (Guo, 2007; Huang, Li, Sun, & Le, 2011). The observation of the dynamic characteristics of algae in Taihu Lake using high temporal resolution satellite data is thus necessary and important. The Geostationary Ocean Color Imager (GOCI), launched by Korea, was decided on as a good choice for this observation (Choi et al., 2012; He et al., 2013; Ruddick et al., 2012; Ryu, Choi, Eom, & Ahn, 2011).

In the study, we establish a simple NIR-red band ratio algorithm of chlorophyll-a concentration (C_{chl-a}) for GOCI data using in situ measurements of remote sensing reflectance and C_{chl-a}, and reveal the dynamic characteristics of C_{chl-a} and phytoplankton bloom by retrieval results of C_{chl-a} from GOCI. This provides reliable satellite observation data to better understand the dynamics of phytoplankton bloom and the factors controlling bloom in Taihu Lake.

2. Data and methods

2.1. Study area

Taihu Lake (30°90′–31°54′N and 119°55.3′–120°59.6′E) is located on the Yangtze River delta, and is a very important drinking water source for the cities of Suzhou, Wuxi and Shanghai. It is the third-largest freshwater lake in China with an area of 2428 km^2 (water surface area is 2338 km^2, island area is 90 km^2), and a mean depth of 1.9 m (Fig. 1). It is influenced by the East Asian monsoon climate. The lake can be separated into seven major segments, including: Meiliang Bay

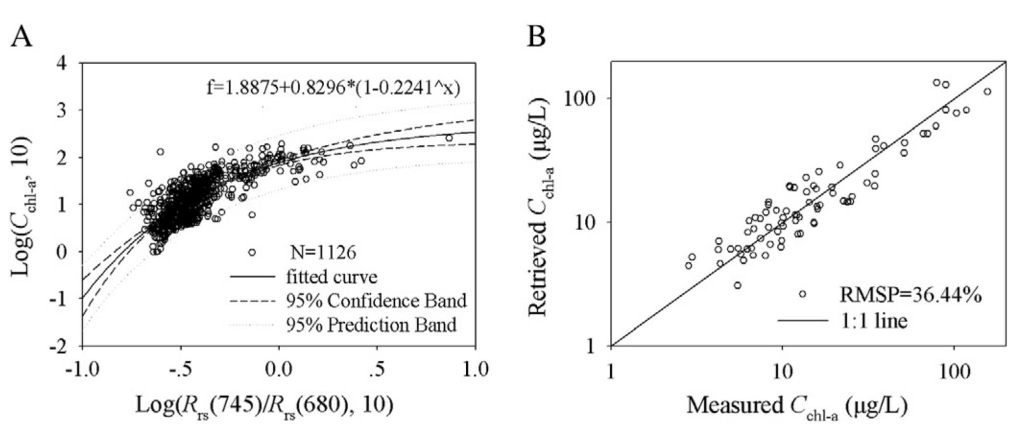

Fig. 2. Calibration and validation of C_{chl-a}NIR-red two-band algorithm.

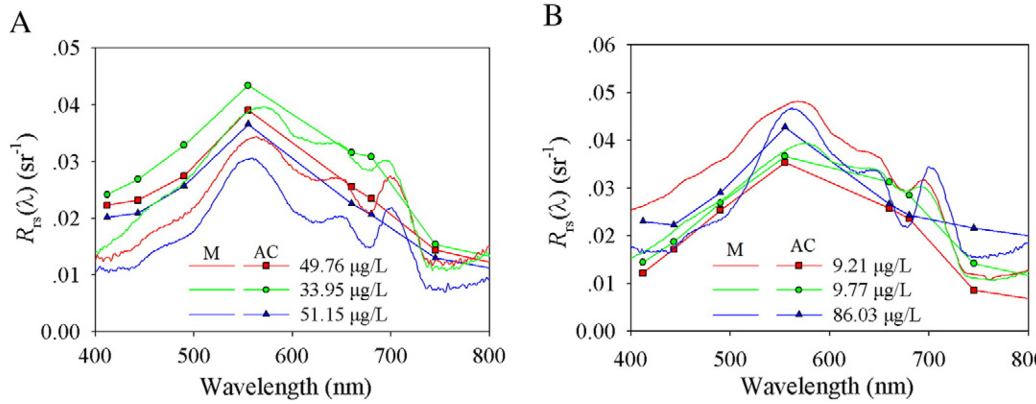

Fig. 3. Atmospheric correction results by 6S model with real-time meteorological parameters. M is measured data, AC is atmospheric correction result, and numbers with μg/L units are $C_{chl\text{-}a}$.

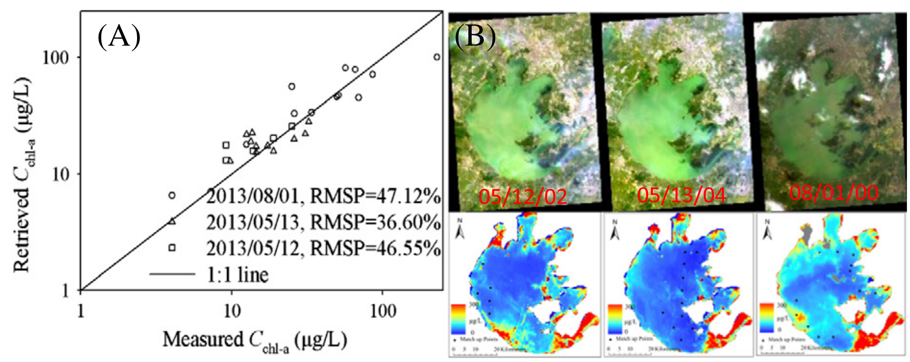

Fig. 4. A is validation of $C_{chl\text{-}a}$NIR-red two-band algorithm by match-up points, B is the synchronous GOCI data on 05/12, 05/13 and 08/01 with the match-up points. The clay in B 2013/08/01/00 is cloud. The RGB image combined from three bands of 745 nm, 555 nm and 412 nm.

(MB), Central Lake (CL), Western Lake (WL), Southwestern Lake (SWL), Gonghu Lake (GL), Eastern Lake (EL) and Eastern Bay (EB) (Fig. 1). The lake became increasingly eutrophic during the 1980s, and its current key issues are hyper-eutrophication and algal blooms (Guo, 2007; Wang and Shi, 2008). The area of blooms has increased significantly, the blooms' duration has lengthened, and their initial blooming date has become earlier (Duan et al., 2009).

2.2. Data sources

2.2.1. Satellite image and data process

GOCI satellite image data with 500 m spatial resolution and 1-hour temporal resolution were used to get the hourly map of $C_{chl\text{-}a}$. Match up data, GOCI level-1b, in 05/12/2013, 05/13/2013, 08/01/2013 and from 08/05/2013 to 08/09/2013 (full clear-sky scenes) were obtained from the Korea Ocean Satellite Center (http://kosc.kordi.re.kr/). The technical software for GOCI (GDPS) is specialized for the ocean, and land information was masked during data processing. Thus, GOCI level-1b data were converted to calibrated radiance data using the self-compiled ENVI–IDL (Interface description language) software package, in which all calibration parameters are from a hierarchical data of the GOCI image. A geometric correction is also included in the software package. Atmospheric influence was corrected (atmospheric correction) based on the radiative transfer calculations from the Second Simulation of the Satellite Signal in the Solar Spectrum (6S model) (Vermote et al., 1997). The continental aerosol type and atmospheric profiles (middle latitude summer type) embedded in the 6S model was used. The MODIS product of aerosol optical thickness surrounding the Taihu Lake was set as input parameters to the 6S model (aerosol concentration). Firstly, the spatial statistic (three pixels around Taihu Lake) mean value of MODIS product of aerosol was calculated and then this mean value (represent the aerosol concentration of whole lake, this process is validated for the full clear-sky scenes) was used to input into 6S model (aerosol concentration in item). Some small improvements to the 6S model were carried out as well, including the addition of real-time atmospheric humidity and pressure. The output parameters from 6S were put into the following equations and calculated the corrected reflectance

$$\begin{aligned} y &= X_a * L - X_b \\ R_{rs} &= y/(1 + X_c * y), \end{aligned}$$

where X_a, X_b and X_c are the output parameters from 6S model, R_{rs} is the atmospheric corrected reflectance, and y is the process variable.

2.2.2. In situ measurement

The in situ measurements of remote sensing reflectance [$R_{rs}(\lambda)$, Sr^{-1}] and chlorophyll-a concentration ($C_{chl\text{-}a}$, μg/L) were conducted from 2004 to 2013. Field measurements, including 1228 samples from 38 cruises, were carried out. The in situ measurement during the period 08/05 to 08/09 in 2013 also contains information on algal species, which were identified with a microscope by manual visual judgment.

$R_{rs}(\lambda)$ measurements were obtained using an analytical spectral device called FieldSpec spectroradiometer (350–1050 nm range, with a

Fig. 5. Spatial variations of $C_{chl\text{-}a}$ mapped by GOCI data during daytime hours from August 6 to August 9. The odd rows are RGB images from three bands of 745 nm, 555 nm and 412 nm. The even rows are GOCI-derived $C_{chl\text{-}a}$. The range of color bar was set to 0–200 μg/L, the GOCI-derived $C_{chl\text{-}a}$ with crimson can be considered algal bloom. Eastern Lake and Eastern Bay were excluded in our analysis so as not to affect our analysis for other segments. For the completeness and aesthetics of figure, areas of Eastern Lake and Eastern Bay were not masked in this study.

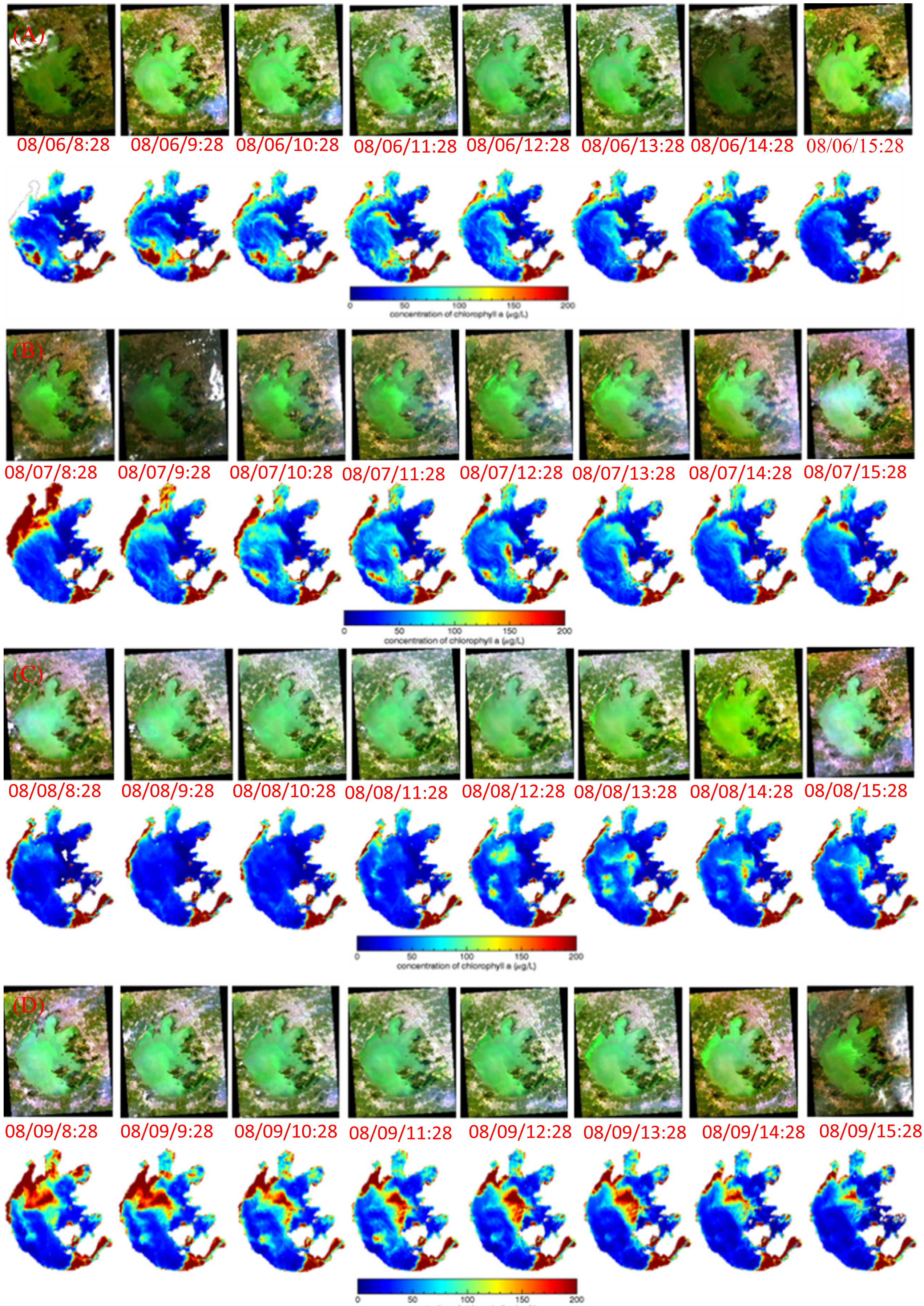
(A)
08/06/8:28
08/06/9:28
08/06/10:28
08/06/11:28
08/06/12:28
08/06/13:28
08/06/14:28
08/06/15:28
0
50
100
150
200
concentration of chlorophyll a (μg/L)
(B)
08/07/8:28
08/07/9:28
08/07/10:28
08/07/11:28
08/07/12:28
08/07/13:28
08/07/14:28
08/07/15:28
0
50
100
150
200
concentration of chlorophyll a (μg/L)
(C)
08/08/8:28
08/08/9:28
08/08/10:28
08/08/11:28
08/08/12:28
08/08/13:28
08/08/14:28
08/08/15:28
0
50
100
150
200
concentration of chlorophyll a (μg/L)
(D)
08/09/8:28
08/09/9:28
08/09/10:28
08/09/11:28
08/09/12:28
08/09/13:28
08/09/14:28
08/09/15:28
0
50
100
150
200
concentration of chlorophyll a (μg/L)

sampling interval of ~1 nm). The spectroradiometer was calibrated by equipment manufacturers every year. $R_{rs}(\lambda)$ was obtained from the measured reflectance radiance of a standard reflectance panel [$L_p(\lambda)$], the upwelling radiance of water [$L_{tw}(\lambda)$] and the downwelling radiance of sky [$L_s(\lambda)$]. The influence factors (such as white hat bubble and solar flare) to measurement of radiance were fully considered and avoided during the period of in situ measurements. Ten spectra were observed for each target and abnormal spectra were removed. The mean value of the rest of the spectra was used to derive $R_{rs}(\lambda)$ (Huang et al., 2011).

Water samples were filtered with GF/C filters (Whatman). The filtered GF/C filters were used to extract chlorophyll-*a* with ethanol (90%) at 80 °C for 6 h in darkness and then analyzed by Shimadzu UV-3600 (Huang, Zou, et al., 2014c). Absorbance difference at 750 and 665 nm, which are before and after removal of phaeopigments by adding hydrochloric acid with 1 mol/L, was used to calculate $C_{chl\text{-}a}$ (Chen, Chen, & Hu, 2006).

2.2.3. Real-time observation data by buoy

The buoy located in Meiliang Bay (marked by a black star in Fig. 1) measured real-time and consecutive data from 08/06/2013 to 08/09/2013 with fifteen-minute intervals. The data include meteorological data (wind speed, wind direction) (Airmar-PB200, USA) and water-current data for different floors (YSI-SonTEK, ADP-1000-1 MHz, USA) and $C_{chl\text{-}a}$. The $C_{chl\text{-}a}$ was measured by fluorometer with a measuring range of 0–100 relative fluorescence units (YSI6600V2-4, USA) at the depths of 0.4 m and 0.8 m.

2.2.4. Application of field measured data

The field measured data was used to calibrate and validate the $C_{chl\text{-}a}$ NIR-red two-band algorithm. In order to get the relatively more robust model, most of measurement data, which included 1126 samples (24 samples with phytoplankton bloom were removed), was used to calibrate the retrieval algorithm of $C_{chl\text{-}a}$. The data (78 samples), collected in summer (2013), were used to validate the retrieval algorithm because the algorithm will be applied to aestival GOCI satellite data. Among of them, seven days of match-up points were found in the data, namely, 05/12, 05/13, 08/01, 08/05, 08/06, 08/07, 08/08 and 08/09 in 2013. Three days of match-up samples (05/12, 05/13 and 08/01) were used to validate the $C_{chl\text{-}a}$ NIR-red two-band algorithm and atmospheric correction method for the GOCI data. The match-up points during the period of 08/05 to 08/09 were used to confirm the validity of GOCI-derived $C_{chl\text{-}a}$ from 08/06/2013 to 08/09/2013 and ensure the correctness of the interpretation of retrieval result. The buoy-observed $C_{chl\text{-}a}$ data during the period of 08/05 to 08/09 was used to validate the capture capability of GOCI for the dynamics of phytoplankton.

2.3. Accuracy assessments

The difference between measured and retrieved value was also normalized to the measured value, called the root mean square error percentage (RMSP). This RMSP was used to assess the accuracy of the NIR-red two-band algorithm. The calculation equation is

$$RMSP = \sqrt{\frac{\sum_{i=1}^{n}[(C_{chl-ar} - C_{chl-am})/C_{chl-am}]^2}{n}}$$

where $C_{chl\text{-}ar}$ and $C_{chl\text{-}am}$ are the retrieved and measured $C_{chl\text{-}a}$.

3. Retrieval model and validation

3.1. Calibration of $C_{chl\text{-}a}$ NIR-red two-band algorithm for simulated GOCI bands

It has been demonstrated that an empirical $C_{chl\text{-}a}$ NIR-red algorithm can be used for estimating $C_{chl\text{-}a}$ in highly turbid productive waters with satisfactory performance (Huang, Zou, et al., 2014; Gilerson et al., 2010; Le et al., 2013; Zhang et al., 2011). Targeted at the NIR-red bands of GOCI (745 nm, 680 nm and 660 nm), a simple NIR-red two-band algorithm was established. The in situ $C_{chl\text{-}a}$ and $R_{rs}(\lambda)$, measured during 37 cruises (1126 points), shows a good relationship between $C_{chl\text{-}a}$ and $R_{rs}(745)/R_{rs}(680)$ at the GOCI bands, which is the average value of $R_{rs}(\lambda)$ according to the width of the GOCI bands (745 ± 10 nm and 680 ± 5 nm) (Huang, Zou, et al., 2014). A total of 1126 samples were used to calibrate the $C_{chl\text{-}a}$ NIR-red two-band algorithm, and 78 samples were used to validate the $C_{chl\text{-}a}$ NIR-red two-band algorithm. The calibration algorithm of $C_{chl\text{-}a}$ is

$$C_{chl-a} = 10^{F(ratio)}, \left(R^2 = 0.71, N = 1126, p<0.001\right)$$
$$F(ratio) = 1.8875 + 0.8296 * \left(1-0.2241^{\log(Rrs(745)/Rrs(680),10)}\right)$$

where, R^2 is the coefficient of determination, N is the sampling number. Almost all the samples (>98%) were in the 95% prediction band (Fig. 2A). The RMSP of validation result between measured and retrieved $C_{chl\text{-}a}$ is 36.44% (Fig. 2B). The test result indicates that the $C_{chl\text{-}a}$ NIR-red two-band algorithm can estimate $C_{chl\text{-}a}$ with acceptable accuracy (Shafique, Autrey, & Fulk, 2001).

3.2. Validation of $C_{chl\text{-}a}$ NIR-red two-band algorithm for GOCI image

3.2.1. Validation of atmospheric correction

To examine the applicability of the $C_{chl\text{-}a}$ NIR-red two-band algorithm to GOCI satellite images, the match-up data (05/12, 05/13, 08/01) in 2013 are used to validate the NIR-red two-band algorithm and atmospheric correction method for the GOCI data. The atmospheric correction results for the match-up points of GOCI show that the performance of the 6S model with real-time meteorological parameters is encouraging, although there is still some uncertainty (Fig. 3). The maximum and minimum relative errors between the measured and atmospheric correction results are −40.65% for $R_{rs}(745)$ with 51.15 μg/L $C_{chl\text{-}a}$ and 3.76% for $R_{rs}(680)$ with 9.77 μg/L $C_{chl\text{-}a}$ (blue line in Fig. 3A and green line in Fig. 3B, respectively). The RMSP of measured and atmospheric correction results [$R_{rs}(745)$ and $R_{rs}(680)$] for all match-up points (total 29 points in Fig. 4A) are 19.80% and 31.24%. However, Dall'Olmo and Gitelson (2005) proposed that some noise caused by the atmosphere can be eliminated by bands ratio. This suggestion is consistent with our results, described below. The maximum and minimum relative error between measured and atmospheric correction results for $R_{rs}(745)$ / $R_{rs}(680)$ are significantly decreased, namely −5.18% for 49.75 μg/L $C_{chl\text{-}a}$ and −23.83% for 9.77 μg/L $C_{chl\text{-}a}$. The RMSP of the measured and atmospheric correction result [$R_{rs}(745)$ / $R_{rs}(680)$] for all match-up points is decreased to 17.61%.

3.2.2. Validation of NIR-red two-band algorithm

The validation of the $C_{chl\text{-}a}$ NIR-red two-band algorithm for match-up points shows that the performance of the $C_{chl\text{-}a}$ NIR-red two-band algorithm is encouraging (Fig. 4A). The RMSPs between measured and retrieved $C_{chl\text{-}a}$ are 47.12%, 36.60% and 46.55% on 08/01, 05/13 and 05/12, respectively. The minimum relative errors between measured and retrieved $C_{chl\text{-}a}$ are −0.28%, 1.55% and 3.01% on 08/01, 05/13 and 05/12, respectively. The maximum relative errors between measured and retrieved $C_{chl\text{-}a}$ are 43.90%, 62.11% and 42.80% on 08/01, 05/13 and 05/12, respectively. The distribution of $C_{chl\text{-}a}$ in Taihu Lake, mapped by synchronous GOCI image data, also suggests that the regional empirical $C_{chl\text{-}a}$ NIR-red two-band algorithm is promising as a means to retrieve $C_{chl\text{-}a}$ for GOCI data (Fig. 4B). High $C_{chl\text{-}a}$ was observed in Meiliang Bay, Zhushan Bay and Gonghu Bay. High $C_{chl\text{-}a}$ was also observed in

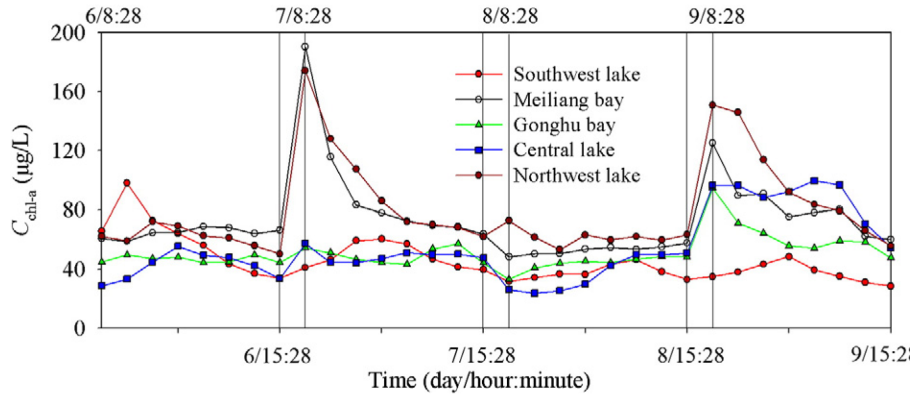

Fig. 6. Hourly variation of C_{chl-a} during daytime hours from August 6 to August 9 for different lake segments.

Southwestern Lake. These are almost consistent with the traditional in situ observations (Huang, Li, Yang, Sun, et al., 2014).

4. Results

4.1. Spatial variations of C_{chl-a} in Taihu Lake mapped by GOCI data

Using the regional C_{chl-a} NIR-red two-band algorithm, we obtained hourly scale maps of C_{chl-a} in Taihu Lake for four consecutive days (Fig. 5). There are large areas of submerged and emergent aquatic plants in Eastern Lake and particularly in Eastern Bay (Ma, Duan, Gu, & Zhang, 2008). The retrieved C_{chl-a} in Eastern Lake and Eastern Bay should not be viewed as accurate due to the influence of seasonal water plants and bottom reflectance (Hu et al., 2010; Ma et al., 2008). Thus, according to the processing method of Hu et al. (2010), Eastern Lake and Eastern Bay were excluded in our analysis so as not to affect our analysis for other segments (Fig. 1A). A diurnal–spatial variation of C_{chl-a} in Taihu Lake is clear. It can even be said that there is a clear hourly-spatial variation of C_{chl-a} in Taihu. The hourly scale maps of C_{chl-a} in the lake can show the dynamics of phytoplankton, including the vertical and horizontal directions. The areas in which C_{chl-a} was greater than 200 μg/L were considered as phytoplankton bloom areas according to the long-term in situ measured C_{chl-a} and investigation. This is feasible and convenient to discuss the distribution and dynamics of phytoplankton bloom in our study periods.

Phytoplankton bloom was observed in Southwestern Lake on August 6 at 8:28 in the morning (Fig. 5A). The phytoplankton bloom became increasingly serious from 8:28 to 9:28 a.m. In the next hour (9:28 to 10:28), however, the surface accumulated phytoplankton bloom wore off significantly and disappeared in the next two hours (10:28 to 12:28). The C_{chl-a} in Southwestern Lake remained lower from 13:28 to 15:28. The C_{chl-a} in Central Lake went through a process from low to high and back to low. The C_{chl-a} in Northwestern Lake (including Zhushan Bay and Meiliang Bay) maintained a high level, and surface accumulated phytoplankton bloom appeared in some areas in Northwestern Lake.

After 17 h, or the next morning, a large area of surface accumulated phytoplankton bloom appeared in Northwestern Lake. The surface accumulated phytoplankton bloom covered almost the entire Zhushan Bay and Meiliang Bay at that point (Fig. 5B, 8:28). The duration of this floating phytoplankton bloom was very short. A large area of surface accumulated phytoplankton bloom in the Northwestern Lake disappeared, except in Zhushan Bay and in the waterfront of Western Lake, during the next 5 h (9:28 to 15:28). However, high C_{chl-a}, in Central Lake and northwestern area of Xishan Island, eventually formed a floating phytoplankton bloom in Central Lake (Fig. 5B, 15:28). From 9:28 to 13:28 on August 7, a patchy surface accumulated phytoplankton bloom appeared in Southwestern Lake (Fig. 5B, 11:28; 12:28). This phytoplankton bloom was hard to monitor from the high time resolution satellite data.

On August 8, in contrast to the large area of floating phytoplankton bloom on the morning of August 7, a small surface accumulated phytoplankton bloom appeared in Zhushan Bay and in the waterfront of Western Lake (Fig. 5C, 8:28). At noon (Fig. 5C, 12:28), a high C_{chl-a} presented in Center and Southwestern Lake. However, this high C_{chl-a} did not form a floating phytoplankton bloom in Southwestern Lake, but a small floating phytoplankton bloom formed in Central Lake (Fig. 5C, 13:28 to 15:28).

The small floating phytoplankton bloom in Zhushan Bay, in the waterfront of Western Lake and in Central Lake (Fig. 5C, 15:28) aggregated into a large area of surface accumulated phytoplankton bloom in the morning of August 8 (Fig. 5D, 8:28). This floating bloom area became even bigger in the next hour. However, the floating bloom area then shrank, although there was still a big area of floating phytoplankton bloom in Central Lake from 12:28 to 13:28.

4.2. Hourly variation of C_{chl-a} for each lake segment

Fig. 6 shows the temporal distributions of pixel average C_{chl-a} for each Taihu Lake segment from GOCI observations. There is an apparent difference during the period of August 6 to August 9. The significant increase of C_{chl-a} in Northwest Lake and Meiliang Bay in the morning from August 7 to August 9 corresponds to a large area of phytoplankton bloom in Fig. 5 (Fig. 5B, D, 8:28). The C_{chl-a} in Northwest Lake and Meiliang Bay maintains a high concentration from August 6 to August 9. Thus, these two segments have a high capacity to form floating phytoplankton bloom in subsequent days. The level of C_{chl-a} in Central Lake is relatively low, except on August 9, which is caused by the appearance of floating phytoplankton bloom. Similarly, high C_{chl-a} in Southwest Lake is accompanied by the appearance of floating phytoplankton bloom on the morning of August 6.

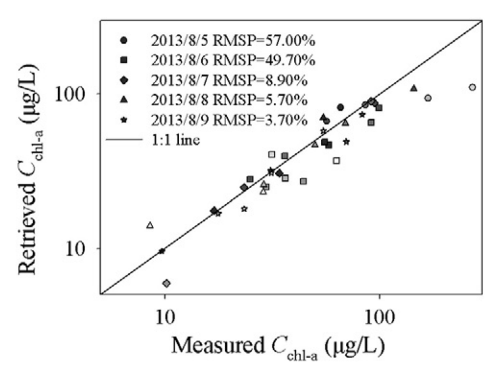

Fig. 7. Comparison of GOCI-derived C_{chl-a} and measured C_{chl-a} for match-up points from August 6 to August 9.

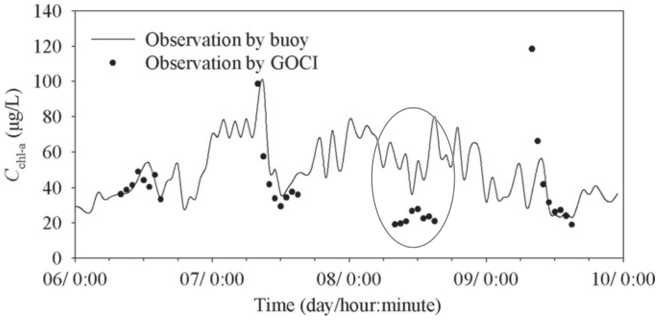

Fig. 8. Comparison of GOCI-derived C_{chl-a} and in situ buoy-measured C_{chl-a} during the daytime, August 6 to August 9. The points in the circle deviated from the buoy monitor.

5. Discussion

5.1. Evaluation of capture capability of GOCI for C_{chl-a}

In order to test the capture capability of C_{chl-a} in Taihu Lake by GOCI satellite image, a comparison of GOCI- retrieved C_{chl-a} with in situ match-up points and buoy measurement of C_{chl-a} was conducted. Fig. 7 shows a comparison of retrieved C_{chl-a} and in situ measurement of match-up points from August 5 to August 9. The RMSPs between measured and retrieved C_{chl-a} are 57.00%, 49.70%, 8.9%, 5.7% and 3.7% on 08/05, 08/06, 08/07, 08/08 and 08/09, respectively. The C_{chl-a} retrieved by GOCI was consistent with the in situ measured C_{chl-a}, which means that GOCI could reliably map the C_{chl-a} in Taihu Lake from 08/05 to 08/09.

How well were the dynamics of phytoplankton captured by GOCI? The diurnal variation of the GOCI-derived C_{chl-a} was a good match with the buoy-observed data, except on August 8 (Fig. 8, marked by ellipse), when the retrieved C_{chl-a} was much lower than that observed by buoy. However, the retrieved C_{chl-a} was much higher than observed by buoy when phytoplankton bloom occurred on August 9 (8:28 and 9:28). There are several potential reasons for this anomaly. The observation depths of the buoy were 0.4 and 0.8 m (middle of water column), but the observation depths of the satellite were different. The difference between satellite and buoy observations will thus become evident when the vertical stratification of C_{chl-a} is very obvious. The diffuse attenuation coefficient in Taihu Lake is very large (Huang et al., 2009; Zhang, Qin, & Chen, 2005), e.g., the diffuse attenuation coefficient (at 490 nm) in summer can reach $6.8 \pm 3.7\ m^{-1}$ (mean value ± standard deviation). Thus, the water constitutes in the deep water level are hard to be monitored in Taihu Lake. Consequently, the underestimation of C_{chl-a} on August 8 may result from the accumulation of phytoplankton in the middle of the water column, which GOCI may not fully detect. Fig. 5C (10:28 to 13:28) also shows that the high C_{chl-a} that appeared at 13:28 was the buoyant phytoplankton from the middle of the water column (there are no floating trails on the surface water). The overestimation of C_{chl-a} on August 9 (8:28 and 9:28) may occur because the phytoplankton is floating on the surface, and there is relatively little phytoplankton in the middle of the water column. Another possible reason for this overestimation is that the buoy (YSI) observed C_{chl-a} is only for algae (chlorophyll-a in the cyanobacteria was not fully detected by buoy) (Seppälä, Ylostalo, & Kaitala, 2007; Simis, Huot, Babin, Seppälä, & Metsamaa, 2012), and the GOCI-derived C_{chl-a} is for all phytoplankton.

5.2. Factors influencing distribution of C_{chl-a}

5.2.1. Growth of phytoplankton affected by nutrients and temperature

It is believed that phytoplankton blooms in Taihu Lake are primarily driven by nutrient levels but are also modulated by meteorological conditions (Hu et al., 2010; Huang, Li, Yang, Sun, et al., 2014; Wilhelm et al., 2011). The in situ measurement data of nutrients show that the total nitrogen (TN) and phosphorus (TP) are 1.866 ± 0.673 mg/L (min–max: 1.013–5.135 mg/L) and 0.156 ± 0.076 mg/L (min–max: 0.029–0.306 mg/L) from August 5 to August 9. The mean ratio of total nitrogen to total phosphorus (TN:TP) is 15.171 ± 8.341 (min–max: 7.569–34.874 mg/L). The C_{chl-a} has a significant positive correlation to total nitrogen and total phosphorus, and the Pearson correlation coefficients are 0.79 and 0.62 ($p < 0.001$) (Fig. 9A). This means that the influence of total nitrogen on C_{chl-a} may stronger than that of total phosphorus on C_{chl-a} during our in situ measurement. This result is similar to that of Paerl et al. (2011). The result, which shows that C_{chl-a} is negatively correlated to TN:TP (Pearson correlation coefficients are −0.40, $p < 0.005$) (Fig. 9B), corresponds to the results of laboratory tests (Kim, Hwang, Shin, An, & Yoon, 2007). These indicate that both total nitrogen and total phosphorus should be reduced to controlled phytoplankton bloom in Taihu Lake. The negative correlation between C_{chl-a} and water temperature (Pearson correlation coefficients are −0.56, $p < 0.001$) (Fig. 9B) indicates that, relative to high temperature, low temperature in summer is much more suited to the phytoplankton growth in Taihu Lake. This may explain the large number of phytoplankton blooms that occurred in the morning with relatively low temperature (Fig. 5).

5.2.2. Drift of phytoplankton bloom affected by hydrodynamic force

In order to characterize the hydrodynamic effect on the phytoplankton distribution, we can reasonably assume that the limitation of TN and TP to phytoplankton growth is minimal at the hourly scale, and that the hourly variation of phytoplankton is the result of modulation by meteorological conditions. The long-distance movement of a large area of phytoplankton on the water surface is rare within a short time period (Fig. 5). This phenomenon was also reported by Reynolds (2006) from dynamic simulation. It may result from low flow velocity. The horizontal laminar flow velocity is not in a fixed direction and is almost less than 10 cm/s from August 6 to August 9 (Fig. 10). This (Fig. 10A, B) indicates

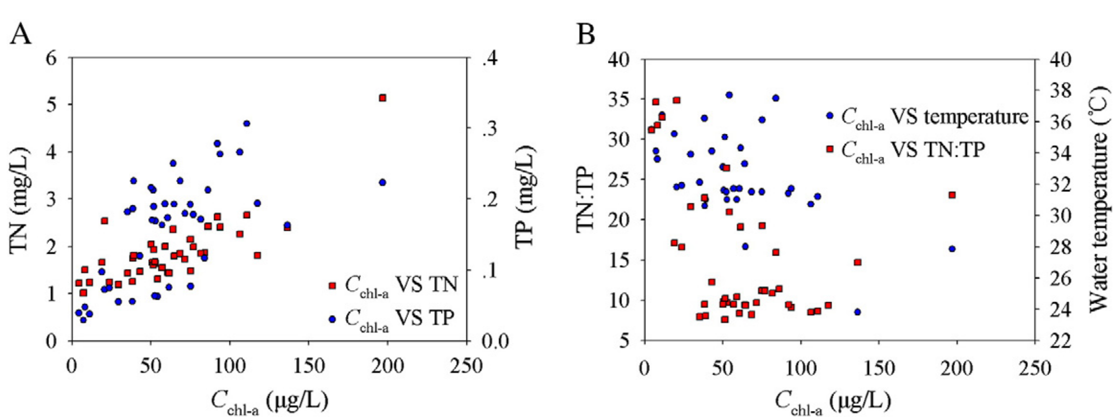

Fig. 9. A is the relationship between C_{chl-a} and nutrients. B is the relationship between C_{chl-a} and temperature, TN:TP.

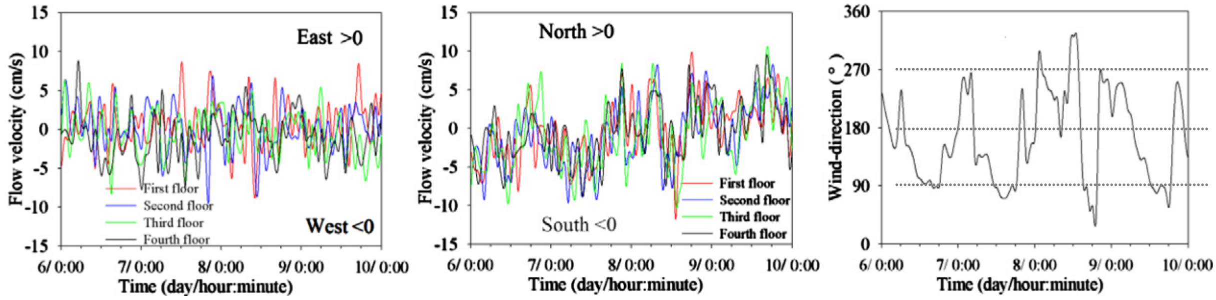

Fig. 10. Buoy-measured flow velocities for different directions and floors (A, B), East > 0 means the direction of flow is east, North > 0 is the same mean with East > 0; and West < 0 means the direction of flow is west, South < 0 is the same mean as West < 0. C is also the wind direction measured by buoy.

that, under this hydrodynamic condition, the phytoplankton can move at most 8640 m for four days (calculated by the maximum flow velocity = 10 cm/s and four days). Thus, the phytoplankton bloom in Zhushan Bay and Meiliang Bay on August 7 had not moved from the phytoplankton in Southwestern Lake on August 6 though laminar flow in the middle of the water column. Fig. 10C shows the wind direction. The flow velocity and direction of water surface are determined primarily by wind speed (within 10 m of the water surface). The floating phytoplankton bloom in Zhushan Bay and Meiliang Bay also did not come from the phytoplankton in Southwestern Lake though the surface current, although the surface current may be much bigger than laminar flow in the middle of the water (Fig. 5, showing that there is almost no floating trail of phytoplankton on the surface water). Wind-driven horizontal drift can contribute to the distribution of phytoplankton bloom, but was not the primary reason for the short-term phytoplankton bloom.

5.2.3. Floating and sinking of phytoplankton affected buoyancy and fluctuation

Cyanophyta were the dominant phytoplankton species in Taihu Lake in the course of this in situ measurement (*cyanophyta*: 97.04% ± 3.24%; *chlorophyta*: 0.79% ± 1.29% and *bacillariophyta*: 2.17% ± 2.47%). Unlike other phytoplankton species, *M. aeruginosa* (one kind of blue algae) can rapidly alter their buoyancy to change their vertical distribution (Sellner et al., 2003). Previous studies have shown that the vertical flow velocity can also significantly affect the vertical distribution of *M. aeruginosa* (Wallace et al., 2000; Fennel & Boss, 2003; Carstensen et al., 2007). Our GOCI observation demonstrated that wind-induced hydrodynamic mixing can carry the *M. aeruginosa* downward. As a result, surface bloom disappeared gradually on August 7 (8:28 to 10:28) and August 9 (9:28 to 15:28) (Fig. 5B, D). The wind threshold value for the disappearance of floating blooms differs among lakes, however, due to differences in depth and morphology, and to the parameters of the lake and the buoyancy of phytoplankton (Binding et al., 2011; Hunter et al., 2008a, 2008b; Webster & Hutchinson, 1994; Wynne et al., 2010). Field (Cao, Kong, Luo, & Shi, 2006) and satellite (MODIS data) (Huang, Li, Yang, Sun, et al., 2014) observations suggest that the phytoplankton bloom disappears when diurnal wind speed exceeds approximately 4 m/s. Huang et al. (2014b) has also described an empirical relationship between wind threshold value (W_t) and dynamic ratio (R_{dr}, is the ratio between square root of lake area and depth), $W_t = 4.8679(R_{dr})^{-0.1}$, according to observations at different lakes. However, in fact, wind threshold value is not a constant in Taihu Lake according to the observation wind speed (Fig. 11A) and GOCI-derived results from August 7 (8:28 to 10:28) and August 9 (9:28 to 15:28). For instance, the floating phytoplankton bloom began disappearing after 8:28 on August 7 with 5.1 m/s wind speed. However, the wind speed was 4.2 m/s after 9:28 on August 9. Additionally, no large area of floating phytoplankton bloom occurred on the morning of August 8 for high wind speed (7.8 m/s) at 21:15 on August 7. The different wind threshold values correspond to different duration times. Thus, the duration time of wind is another important factor. Fig. 11B shows the vertical flow velocity measured by buoy between −1.7 cm/s and 2.1 cm/s. This velocity is bigger than the buoyancy of *M. aeruginosa* (0.9 cm/s) calculated by Huang et al. (2014a), and easily pushes the algae (with 0.9 cm/s buoyancy) down.

6. Conclusions

Based on the GOCI-derived $C_{chl\text{-}a}$, in situ measured water quality parameters and buoy-measured $C_{chl\text{-}a}$, some major findings can be made from this study. First, the NIR-red two-band algorithm and 6S model with real-time atmospheric humidity and pressure can be applied to retrieve $C_{chl\text{-}a}$ in Taihu Lake by GOCI data. Second, GOCI-derived $C_{chl\text{-}a}$ can capture the spatial variation and dynamic characteristics of $C_{chl\text{-}a}$ and phytoplankton bloom in the lake. Third, nutrients are required for phytoplankton bloom in the lake; the vertical movement induced by both phytoplankton buoyancy and fluctuation govern the hourly spatial

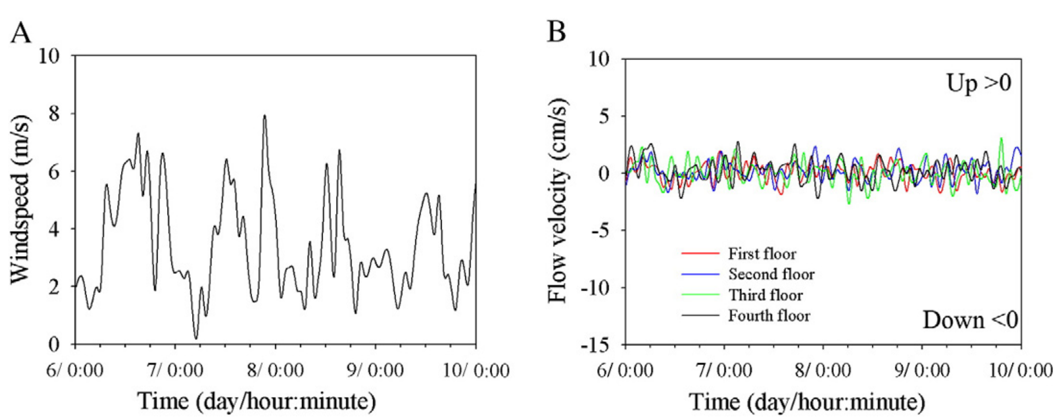

Fig. 11. A is the wind speed measured by buoy from August 6 to August 9. B is buoy-measured flow velocities for different floors, Up > 0 means the direction of flow is an upwelling current, and Down < 0 means the direction of flow is a downwelling current.

and temporal variation of phytoplankton, and the horizontal movement of phytoplankton is significant over the long term, but spatially and temporally limited in the short term.

Acknowledgments

This study was supported by the National Natural Science Foundation of China (Grant Nos. 41201325, 41271343), the Ph.D. Program Foundation of the Ministry of Education of China (Grant No. 20123207120017), Project Funded by the Priority Academic Program Development of Jiangsu Higher Education Institutions. Thanks to the Korea Ocean Satellite Center for the sharing of GOCI data and we appreciate Tingwei Cui for the help of data download. We are grateful to Rebecca for the language editing, and deeply thank the two anonymous reviewers and associate editor Professor Tiit Kutser for their very helpful comments.

References

Abell, J.M., Ozkundakci, D., & Hamilton, D.P. (2010). Nitrogen and phosphorus limitation of phytoplankton growth in New Zealand lakes: Implications for eutrophication control. *Ecosystems*. http://dx.doi.org/10.1007/s10021-010-9367-9.

Binding, C.E., Greenberg, T.A., & Bukata, R.P. (2011). Time series analysis of algal blooms in Lake of the Woods using the MERIS maximum chlorophyll index. *Journal of Plankton Research*, *33*(12), 1847–1852.

Cao, H.S., Kong, F.X., Luo, L.C., & Shi, X.L. (2006). Effects of wind and wind-induced waves on vertical phytoplankton distribution and surface blooms of *Microcystis aeruginosa* in Lake Taihu. *Journal of Freshwater Ecology*, *21*, 231–238.

Carstensen, J., Henriksen, P., & Heiskanen, A.S. (2007). Summer algal blooms in shallow estuaries: Definition, mechanisms, and link to eutrophication. *Limnology and Oceanography*, *52*(1), 370–384.

Chen, Y.W., Chen, K.N., & Hu, Y.H. (2006). Discussion on possible error for phytoplankton chlorophyll-a concentration analysis using hot-ethanol extraction method. *Journal of Lake Science*, *18*, 550–552.

Choi, J.K., Park, Y.J., Ahn, J.H., Lim, H.S., Eom, J., & Ryu, J.H. (2012). GOCI, the world's first geostationary ocean color observation satellite, for the monitoring of temporal variability in coastal water turbidity. *Journal of Geophysical Research, Oceans*, *117*(C9). http://dx.doi.org/10.1029/2012JC008046.

Cloern, J.E. (2001). Review our evolving conceptual model of the coastal eutrophication problem. *Marine Ecology Progress Series*, *210*, 223–253.

Conley, D.J., Paerl, H.W., Howarth, R.W., Boesch, D.F., Seitzinger, S.P., Havens, K.E., et al. (2009). Controlling eutrophication: Nitrogen and phosphorus. *Science*, *323*, 1014–1015.

Dall'Olmo, G., & Gitelson, A.A. (2005). Effect of bio-optical parameter variability on the remote estimation of chlorophyll-a concentration in turbid productive waters: Experimental results. *Applied Optics*, *44*(3), 412–422.

Duan, H.T., Ma, R.H., Xu, X.F., Kong, F.X., Zhang, S.X., Kong, W.J., et al. (2009). Two decade reconstruction of algal blooms in China's Lake Taihu. *Environmental Science and Technology*, *43*, 3522–3528.

Dzialowski, A.R., Wang, S.H., Lim, N.C., Beury, J.H., & Huggins, D.G. (2008). Effects of sediment resuspension on nutrient concentrations and algal biomass in reservoirs of the Central Plains. *Lake and Reservoir Management*, *24*, 313–320.

Fennel, K., & Boss, E. (2003). Subsurface maxima of phytoplankton and chlorophyll: Steady-state solutions from a simple model. *Limnology and Oceanography*, *48*(4), 1521–1534.

Gilerson, A. A., Gitelson, A. A., Zhou, J., Gurlin, D., Moses, W. J., Ioannou, I., & Ahmed, S. A. (2010). Algorithms for remote estimation of chlorophyll-a in coastal and inland waters using red and near-infrared bands. *Optics Express*, *18*, 24109–24125.

Gower, J., King, S., Borstad, G., & Brown, L. (2005). Detection of intense plankton blooms using the 709 nm band of the MERIS imaging spectrometer. *International Journal of Remote Sensing*, *26*(9), 2005–2012.

Guo, L. (2007). Doing battle with the green monster of Lake Taihu. *Science*, *317*, 1166.

He, X.Q., Bai, Y., Pan, D.L., Huang, N.L., Dong, X., Chen, J.S., et al. (2013). Using geostationary satellite ocean color data to map the diurnal dynamics ofsuspended particulate matter in coastal waters. *Remote Sensing of Environment*, *133*, 225–239.

Hu, C.H. (2009). A novel ocean color index to detect floating algae in the global oceans. *Remote Sensing of Environment*, *113*, 2118–2129.

Hu, C.H., Frank, E., Karger, M., Taylor, C., Carder, K.L., Kelble, C., et al. (2005). Red tide detection and tracing using MODIS fluorescence data: A regional example in SW Florida coastal waters. *Remote Sensing of Environment*, *97*, 311–321.

Hu, C.H., Lee, Z.P., Ma, R.H., Yu, K., Li, D.Q., & Shang, S.L. (2010). Moderate Resolution Imaging Spectroradiometer (MODIS) observations of cyanobacteria blooms in Taihu Lake, China. *Journal of Geophysical Research*, *115*, C04002. http://dx.doi.org/10.1029/2009JC005511.

Huang, C.C., Li, Y.M., Sun, D.Y., & Le, C.F. (2011). Retrieval of *Microcystis aentginosa* percentage from high turbid and eutrophia inland water: A case study in Taihu Lake. *IEEE Transactions on Geoscience and Remote Sensing*, *49*(10), 4049–4100.

Huang, C.C., Li, Y.M., Sun, D.Y., Le, C.F., Wu, L., Wang, L., et al. (2009). Characteristics of the diffuse attenuation coefficient and its impact on aquatic ecology environment. *Environmental Sciences*, *30*(2), 348–355 (English abstract).

Huang, C.C., Li, Y.M., Yang, H., Li, J.S., Chen, X., Sun, D.Y., et al. (2014). Assessment of water constituents in highly turbid productive water by optimization bio-optical retrieval model after optical classification. *Journal of Hydrology*, *519*, 1572–1583.

Huang, C.C., Li, Y.M., Yang, H., Sun, D.Y., Yu, Z.Y., Zhang, Z., et al. (2014a). Detection of algal bloom and factors influencing its formation in Taihu Lake from 2000 to 2011 by MODIS. *Earth Environmental Science*, *71*, 3705–3714.

Huang, C.C., Wang, X.L., Yang, H., Li, Y.M., Wang, Y.H., Chen, X., et al. (2014b). Satellite data regarding the eutrophication response to human activities in the plateau lake Dianchi in China from 1974 to 2009. *Science of the Total Environment*, *485–485*, 1–11.

Huang, C.C., Zou, J., Li, Y.M., Yang, H., Shi, K., Li, J.S., et al. (2014c). Assessment of NIR-red algorithms for observation of chlorophyll-a in highly turbid inland waters in China. *ISPRS Journal of Photogrammetry and Remote Sensing*, *93*, 29–39.

Hunter, P.D., Tyler, A.N., Willby, N.J., & Gilvear, D.J. (2008a). The spatial dynamics of vertical migration by *Microcystis aeruginosa* in a eutrophic shallow lake: A case study using high spatial resolution time-series airborne, remote sensing. *Limnology and Oceanography*, *53*(6), 2391–2406.

Hunter, P.D., Tyler, A.N., Willby, N.J., & Gilvear, D.J. (2008b). The spatial dynamics of vertical migration by *Microcystis aeruginosa* in a eutrophic shallow lake: A case study using high spatial resolution time-series airborne remote sensing. *Limnology and Oceanography*, *53*, 2391–2406.

Jöhnk, K. D., Huisman, J., Sommeijer, B., Sharples, J., Visser, P. M., & Stroom, J. (2008). Summer heatwaves promote blooms of harmful cyanobacteria. *Global Change Biology*, *14*, 495–512.

Kim, H.S., Hwang, S.J., Shin, J.K., An, K.G., & Yoon, C.G. (2007). Effects of limiting nutrients and N:P ratios on the phytoplankton growth in a shallow hypertrophic reservoir. *Hydrobiologia*, *581*, 255–267.

Le, C.F., Li, Y.M., Zha, Y., Sun, D.Y., Huang, C.C., & Lu, H. (2009). A four-band semi-analytical model for estimating chlorophyll a in highly turbid lakes: The case of Taihu Lake, China. *Remote Sensing of Environment*, *113*, 1175–1182.

Le, C. F., Hu, C. M., Cannizzaro, J., English, D., Muller-Karger, F., & Lee, Z. P. (2013). Evaluation of chlorophyll-a remote sensing algorithms for an optically complex estuary. *Remote Sensing of Environment*, *129*, 75–89.

Liu, X., Wang, M., & Shi, W. (2009). A study of a Hurricane Katrina—Induced phytoplankton bloom using satellite observations and model simulations. *Journal of Geophysical Research*, *114*(C03023). http://dx.doi.org/10.1029/2008JC004934.

Ma, R.H., Duan, H.T., Gu, X.H., & Zhang, S.X. (2008). Detecting aquatic vegetation changes in Taihu Lake, China using multi-temporal satellite imagery. *Sensors*, *8*, 3988–4005.

Michalak, A.M., Anderson, E.J., Beletsky, D., Boland, S., Bosch, N.S., Bridgeman, T.B., et al. (2013). Record-setting algal bloom in Lake Erie caused by agricultural and meteorological trends consistent with expected future conditions. *Proceedings of the National Academy of Sciences of the United States of America (PNAS)*, *110*(16), 6448–6452.

Moore, S.K., Trainer, V.L., Mantua, N.J., Parker, M.S., Laws, E.A., Backer, L.C., et al. (2008). Impacts of climate variability and future climate change on harmful algal blooms and human health. *Environmental Health*, *7*(2), S4.

Moreno-Ostos, E., Cruz-Pizarro, L., Basanta, A., & George, D.G. (2009). The influence of wind-induced mixing on the vertical distribution of buoyant and sinking phytoplankton species. *Aquatic Ecology*, *43*, 271–284.

Odermatt, D., Pomati, F., Pitarch, J., Carpenter, J., Kawka, M., Schaepman, M., et al. (2012). MERIS observations of phytoplankton blooms in a stratified eutrophic lake. *Remote Sensing of Environment*, *126*, 232–239.

Paerl, H.W., & Huisman, J. (2009). Climate change: A catalyst for global expansion of harmful cyanobacterial blooms. *Environmental Microbiology Reports*, *1*(1), 27–37.

Paerl, H. W., Xu, H., McCarthy, M. J., Zhu, G., Qin, B., & Li, Y. (2011). Gardner., Controlling harmful cyanobacterial blooms in a hyper-eutrophic lake (Lake Taihu, China): The need for a dual nutrient (N & P) management strategy. *Water Research*, *45*, 1973–1983.

Qin, B.Q., Xu, P.Z., Wu, Q.L., Luo, L.C., & Zhang, Y.L. (2007). Environmental issues of Lake Taihu, China. *Hydrobiologia*, *581*, 3–14.

Qin, B.Q., Zhu, G.W., Zhang, L., Luo, L.C., Gao, G., & Gu, B.H. (2006). Estimation of internal nutrient release in large shallow Lake Taihu, China. *Science in China Series D*, *49*, 38–50.

Rabalais, N.N. (2004). Eutrophication. Chapter 21 In A.R. Robinson, J. McCarthy, & B.J. Rothschild (Eds.), *The global coastal ocean: Multiscale interdisciplinary processes. The sea*, *13*. (pp. 819–865). Cambridge, MA: Harvard University Press.

Reynolds, C.S. (2006). *The ecology of phytoplankton*. Cambridge: Cambridge University Press, 535.

Ruddick, K., Vanhellemont, Q., Yan, J., Neukermans, G., Wei, G.M., & Shang, S.L. (2012). Variability of suspended particulate matter in the Bohai Sea from the Geostationary Ocean Color Imager (GOCI). *Ocean Science Journal*, *47*(3), 331–345.

Ryu, J.H., Choi, J.K., Eom, J., & Ahn, J.H. (2011). Temporal variation in Korean coastal waters using Geostationary Ocean Color Imager. *Journal of Coastal Research*, *64*, 1731–1735.

Schindler, D.W., Hecky, R.E., Findlay, D.L., Stainton, M.P., Parker, B.R., Paterson, M., et al. (2008). Eutrophication of lakes cannot be controlled by reducing nitrogen input: Results of a 37 year whole ecosystem experiment. *Proceedings of the National Academy of Sciences of the United States of America (PNAS)*, *105* (11254e11258).

Schindler, D.W., Hecky, R.E., & McCullough, G.K. (2012). The rapid eutrophication of Lake Winnipeg: Greening under global change. *Journal of Great Lakes Research*, *38*(3), 6–13.

Sellner, K. G., Doucette, G. J., & Kirkpatrick, G. J. (2003). Harmful algal blooms: causes, impacts and detection. *J. Ind. Microbiol Biotechnol*, *30*, 383–406. http://dx.doi.org/10.1007/s10295-003-0074-9.

Seppälä, J., Ylostalo, P., Kaitala, S., Hällfors, S., Raateoja, M., & Maunula, P. (2007). Ship-of-opportunity based phycocyanin fluorescence monitoring of the filamentous cyanobacteria bloom dynamics in the Baltic Sea. *Estuarine, Coastal and Shelf Science*, *73*, 489–500.

Shafique, N.A., Autrey, B.C., & Fulk, F. (2001). Hyperspectral narrow wavebands selection for optimizing water quality monitoring on the Great Miami River, Ohio. *Journal of Spatial Hydrology*, *1*(1), 1–22.

Shanmugam, P. (2011). A new bio-optical algorithm for the remote sensing of algal blooms in complex ocean waters. *Journal of Geophysical Research*, *116*, C04016. http://dx.doi.org/10.1029/2010JC006796.

Simis, S.G.H., Huot, Y., Babin, M., Seppälä, J., & Metsamaa, L. (2012). Optimization of variable fluorescence measurements of phytoplankton communities with cyanobacteria. *Photosynthesis Research*, *112*, 13–30.

Stumpf, R.P., Wynne, T.T., Baker, D.B., & Fahnenstiel, G.L. (2012). Interannual variability of cyanobacterial blooms in Lake Erie. *PLoS ONE*, *7*(8), e42444. http://dx.doi.org/10.1371/journal.pone.0042444.

Vermote, E., Tanre, D., Deuze, J., Herman, M., & Morcette, J. (1997). Secondsimulation of the satellite signal in the solar spectrum, 6S: An overview. *IEEE Transactions on Geoscience and Remote Sensing*, *35*, 675–686.

Wallace, B.B., Bailey, M.C., & Hamilton, D.P. (2000). Simulation of vertical position of buoyancy regulating *Microcystis aeruginosa* in a shallow eutrophic lake. *Aquatic Sciences*, *62*, 320–333.

Wang, M., & Shi, W. (2008). Satellite-observed algae bloom in China's Lake Taihu. *EOS Trans AGU*, *89*, 201–202.

Wang, M.H., Shi, W., & Tang, J.W. (2011). Water property monitoring and assessment for China's inland Lake Taihu from MODIS-Aqua measurements. *Remote Sensing of Environment*, *115*, 841–854.

Webster, I.T., & Hutchinson, P.A. (1994). Effect of wind on the distribution of phytoplankton cells in lakes revisited. *Limnology and Oceanography*, *39*(2), 365–373.

Wilhelm, S.W., Farnsley, S.E., LeCleir, G.R., Layton, A.C., Satchwell, M.F., DeBruyn, J.M., et al. (2011). The relationships between nutrients, cyanobacterial toxins and the microbial community in Taihu (Lake Tai), China. *Harmful Algae*, *10*, 207–215.

Wong, K.T.M., Lee, J.H.W., & Hodgkiss, I.J. (2007). A simple model for forecast of coastal algal blooms. *Estuarine, Coastal and Shelf Science*, *74*, 175–196.

Wu, X.D., & Kong, F.X. (2009). Effects of light and wind speed on the vertical distribution of *Microcystis aeruginosa* colonies of different sizes during a summer bloom. *International Review of Hydrobiology*, *94*, 258–266.

Wu, T.F., Qin, B.Q., Zhu, G.W., Luo, L.C., Ding, Y.Q., & Bian, G.Y. (2013). Dynamics of cyanobacterial bloom formation during short-term hydrodynamic fluctuation in a large shallow, eutrophic, and wind-exposed Lake Taihu, China. *Environmental Science and Pollution Research*, *20*, 8546–8556.

Wynne, T.T., Stumpf, R.P., Tomlinson, M.C., & Dyble, J. (2010). Characterizing a cyanobacterial bloom in western Lake Erie using satellite imagery and meteorological data. *Limnology and Oceanography*, *55*(5), 2025–2036.

Xu, H., Paerl, H.W., Qin, B.Q., Zhu, G.W., & Gao, G.G. (2010). Nitrogen and phosphorus inputs control phytoplankton growth in eutrophic Lake Taihu, China. *Limnology and Oceanography*, *55*, 420–432.

Zhang, M., Duan, H.T., Shi, X.L., Yu, Y., & Kong, F.X. (2012). Contributions of meteorology to the phenology of cyanobacterial blooms: Implications for future climate change. *Water Research*, *46*, 442–452.

Zhang, Y.L., Qin, B.Q., & Chen, W.M. (2005). Attenuation of photosynthetically available radiance (PAR) in Meilaing Bay under different winds and waves. *Chinese Journal of Applied Ecology*, *16*(6), 1133–1137 (English abstract).

Zhang, Y. Z., Lin, H., Chen, C. Q., Chen, L. D., Zhang, B., & Gitelson, A. A. (2011). Estimation of chlorophyll-a concentration in estuarine waters: case study of the Pearl River estuary, South China Sea. *Environmental Research Letters*, *6*, 024016.